Vlasov simulations of wave-particle interactions and turbulence in magnetized plasma

IRF-U, Uppsala, 16 November 2016

Bengt Eliasson

ABP Group, Physics Department, SUPA
Strathclyde University, UK

Collaborators:
D. C. Speirs, T. Heelis, Strathclyde University, UK
K. Papadopoulos, A. Najmi, G. Milikh, X. Shao, U. Maryland
T. B. Leyser, IRF-U, Uppsala, Sweden
L. Daldorff, NASA Goddard Space Flight Center & Johns Hopkins U. APL, MD
M. Lazar, University of Leuven, Belgium

Outline

A. Artificial aurora and descending ionospheric fronts in recent heating experiments

B. High-frequency turbulence induced by large amplitude electromagnetic waves

C. Anomalous absorption on striations

D. Stochastic electron heating by large amplitude electron Bernstein waves

E. Electron acceleration by strong Langmuir turbulence, ionization of neutral gas

F. Summary

High Frequency Active Auroral Research Program (HAARP)

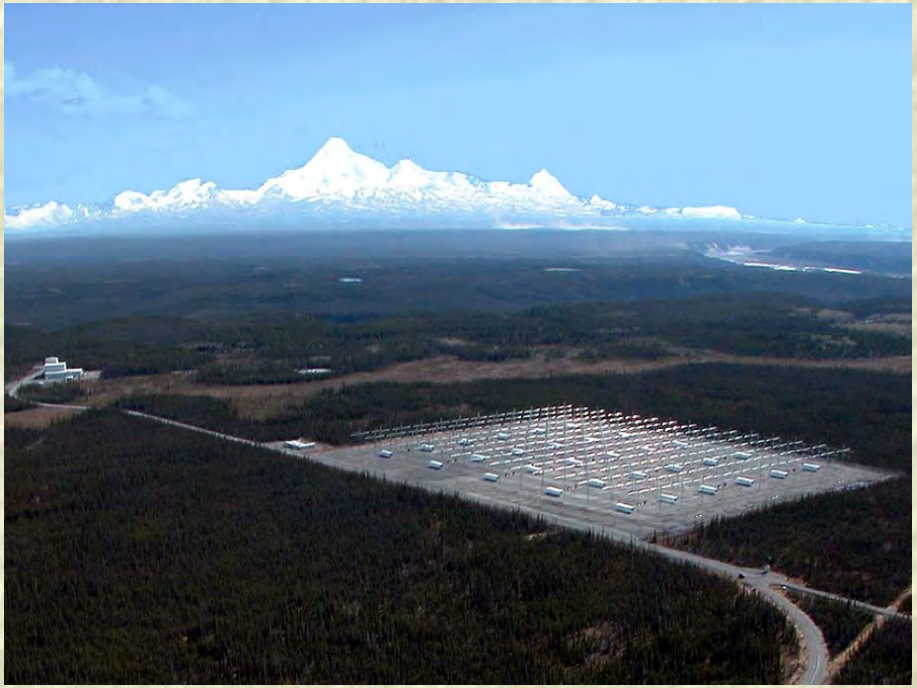

HAARP research station, near Gakona, Alaska

Established 1993, last major upgrade 2007.

Observations of descending aurora above HAARP

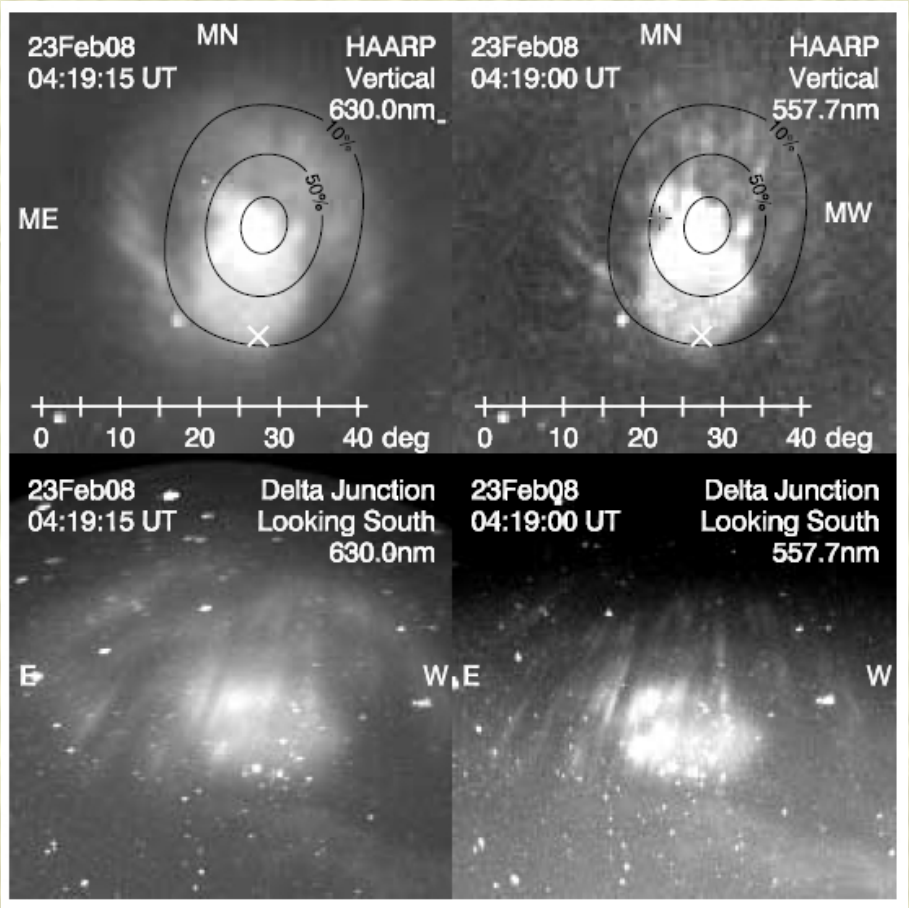

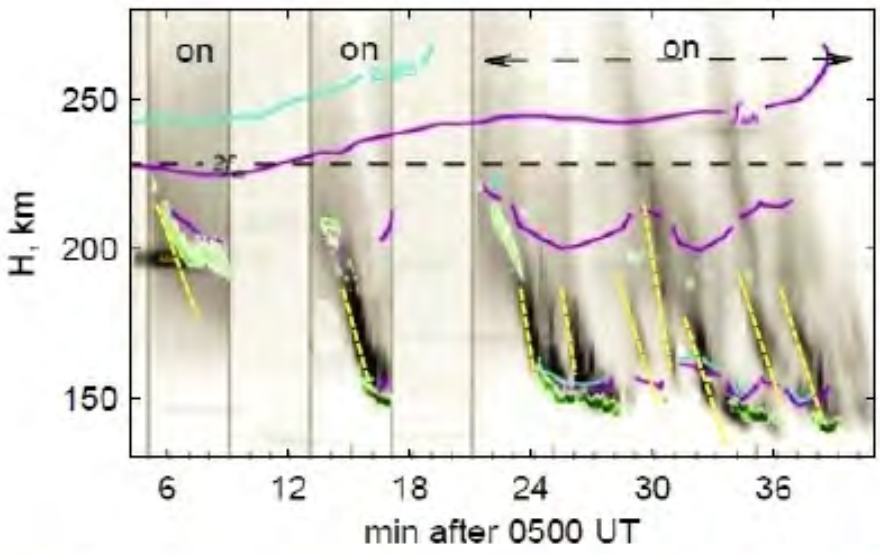

Time-vs-altitude plot of 557.7 nm optical emissions along *B* with contours showing the altitudes where *fp =2.85 MHz (blue), UHR= 2.85* MHz (violet), and $2f_{ce}$ = *2.85 MHz (dashed white). Horizontal blips* are stars. **Shown in green is the Ion Acoustic Line intensity.**

✓**the artificial plasma near h_{min} was quenched several times.**

Pedersen, Gustavsson, Mishin *et al.*, Geophys. Res. Lett., 36, L18107 (2009).
Pedersen, Mishin *et al.*, Geophys. Res. Lett., 37, L02106 (2010).
Mishin & Pedersen, Geophys. Res. Lett., 38, L01105 (2011).

Rays of ordinary (O) mode waves

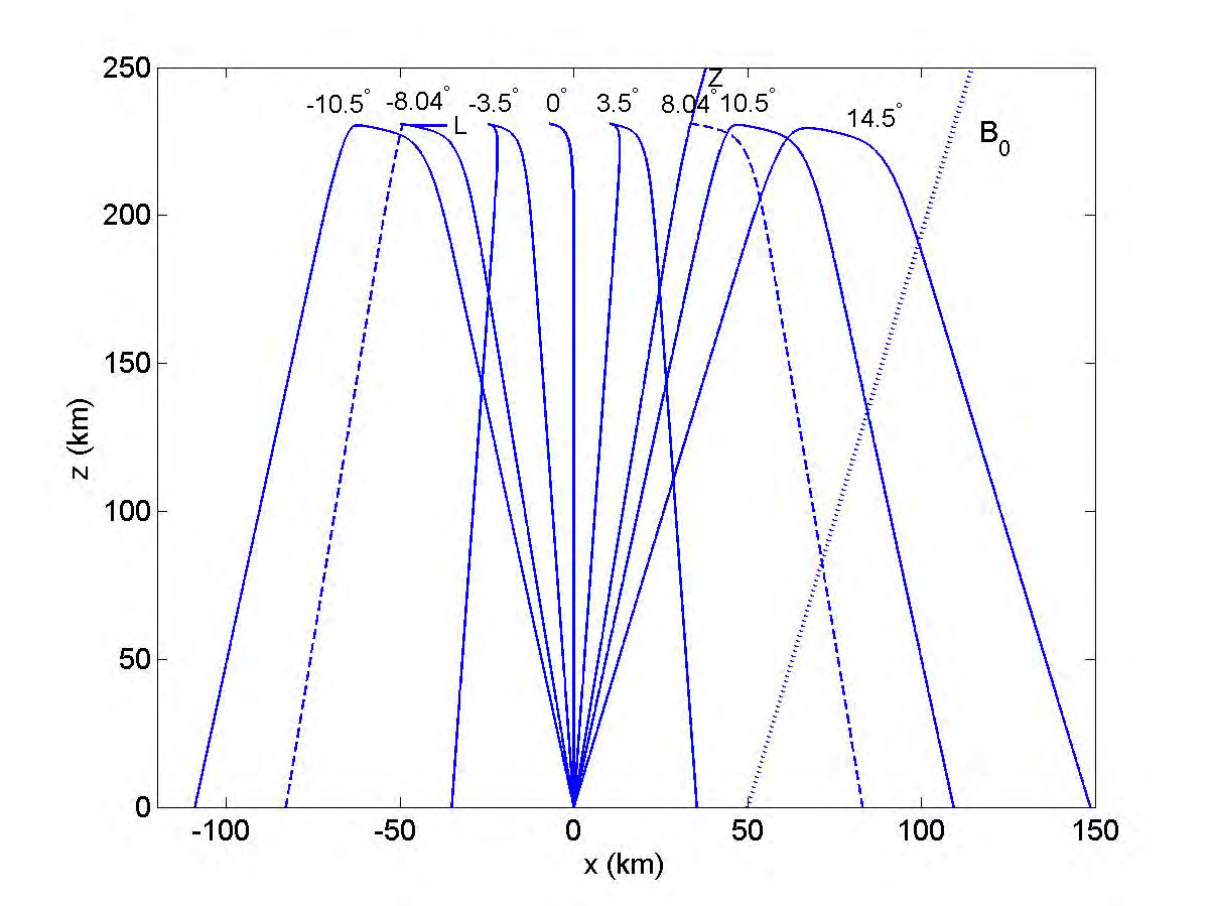

Ray-tracing

$$\frac{d\mathbf{k}}{dt} = -\nabla_{\mathbf{r}}\omega$$

$$\frac{d\mathbf{r}}{dt} = \nabla_{\mathbf{k}}\omega$$

Appleton-Hartree dispersion relation gives $\omega(\mathbf{k}, \mathbf{r})$

Magnetic field $\mathbf{B}_0 = 5 \times 10^{-5}\,\mathrm{T}$, tilted $\theta = 14.5°$ to vertical. Electron cyclotron frequency $f_{ce} = 1.4\,\mathrm{MHz}$.

$f_0 = 3.2$ MHz transmitted frequency, ~ 100 m vacuum wavelength.

Ordinary mode waves are reflected near the critical layer where $\omega = \omega_{pe}$.

Rays closeup near reflection point

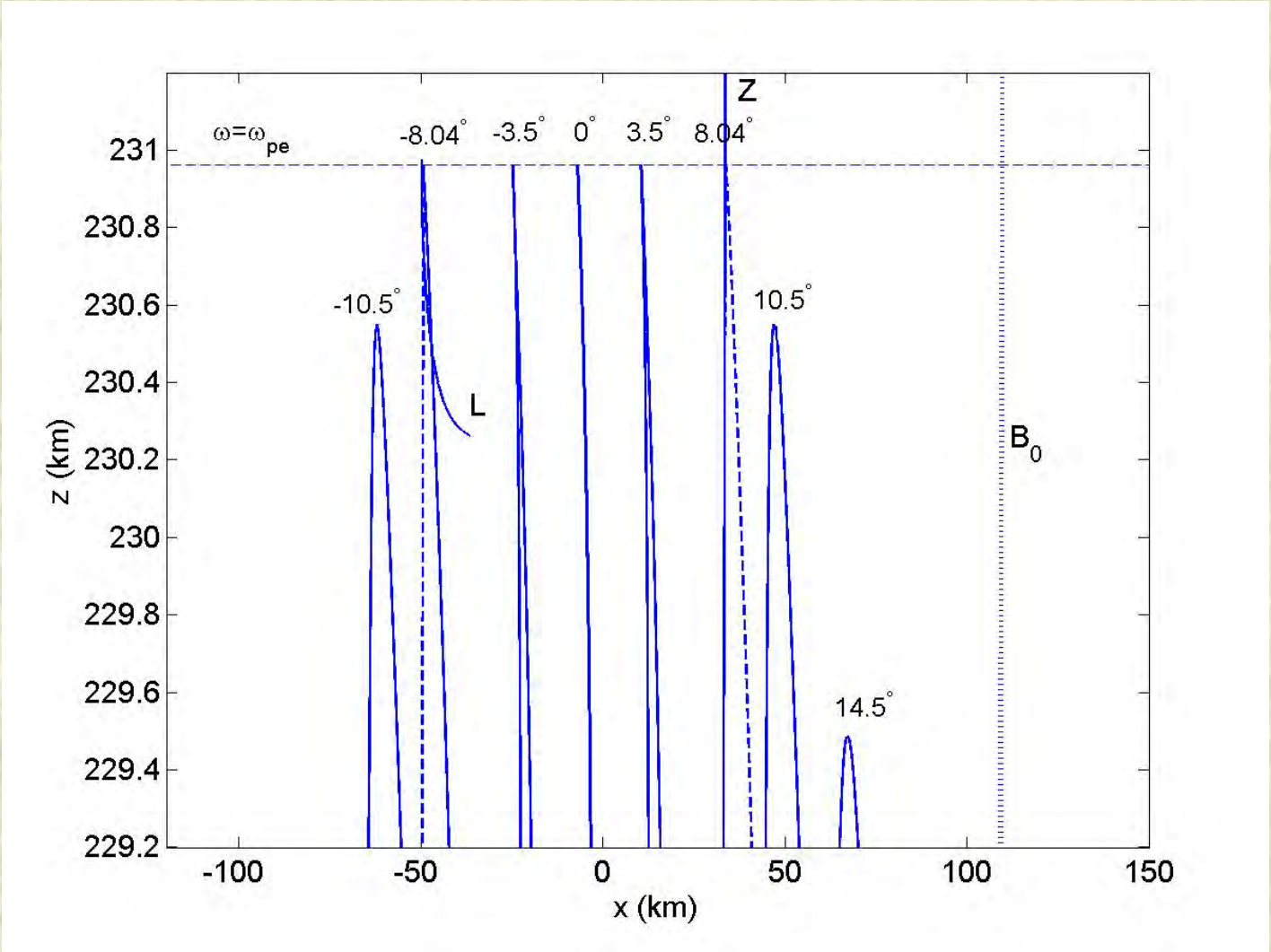

Rays within the Spitze region $\chi_S = \pm \arcsin[\sqrt{Y/(1+Y)}\sin(\theta)] \approx \pm 8.04°$ reach the critical layer.

Anomalous absorption of electromagnetic waves

- It is observed that O mode radio waves injected along the magnetic field lines become absorbed by the ionosphere after about one second of heating
- Happens when the transmitted frequency is below the maximum upper hybrid frequency of the ionosphere
- Believed to be due to mode conversion to upper hybrid waves on density striations created due to thermal instability

Conversion O mode to upper hybrid waves

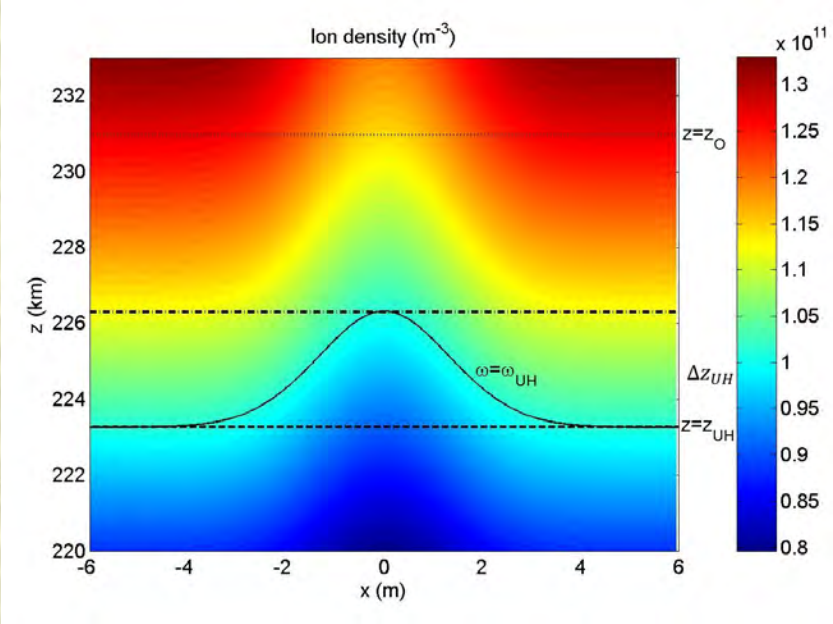

- O mode waves reflected at critical altitude $z = z_O$ where $\omega = \omega_{pe}$.
- Solid lines: Where locally $\omega = \omega_{UH}$ mode conversion O mode to upper hybrid waves can take place.
- Full-wave simulations to study the coupling between O mode and UH waves. Coordinate system such that z-axis along the magnetic field.

Eliasson & Papadopoulos, Geophys. Res. Lett. **42**, 2603 (2015).

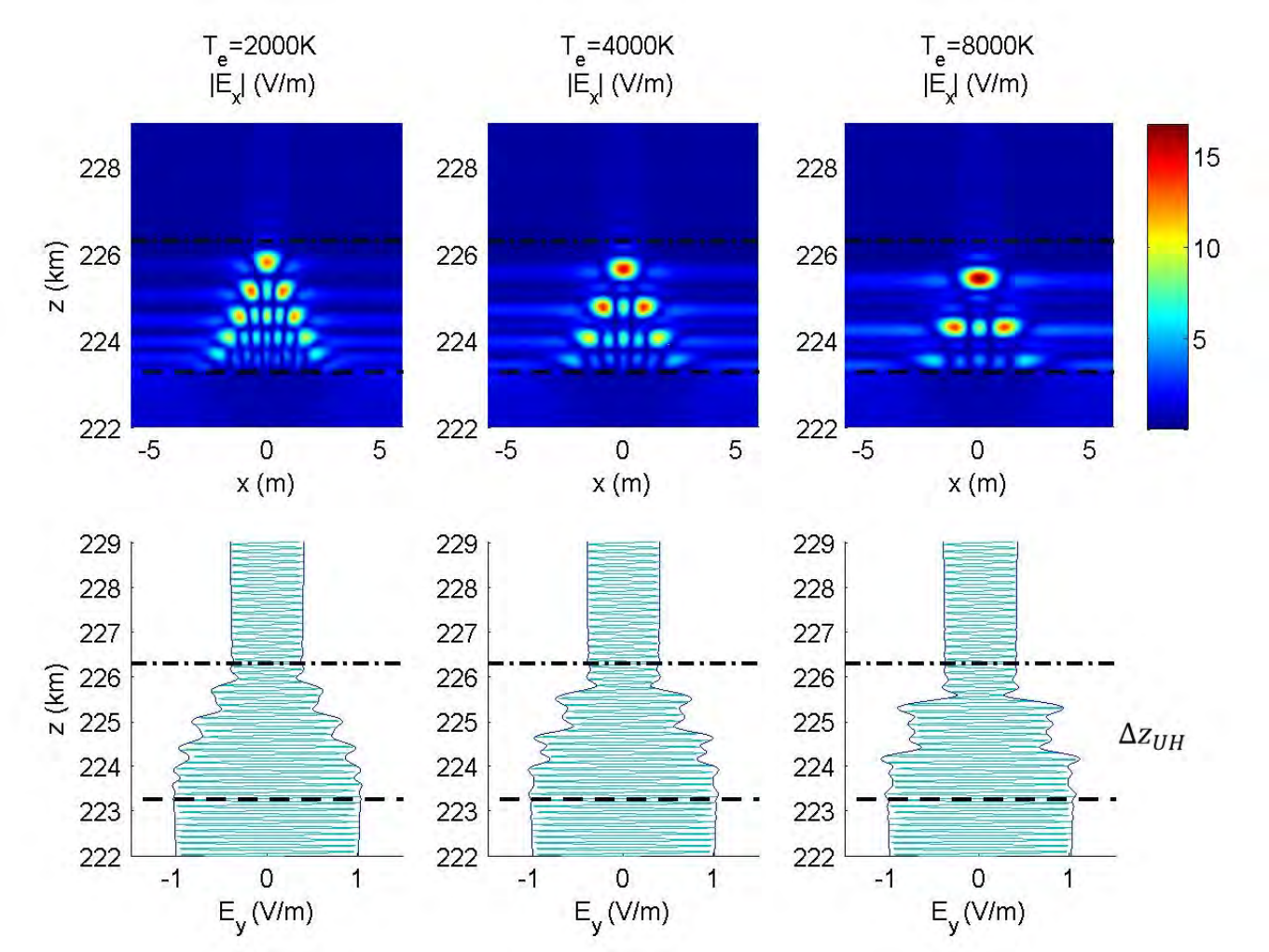

Excitations of UH waves (top) at quantized heights where UH frequency matches resonance frequency (Sturm-Liouville problem). Absorption of O mode wave (bottom) not dependent on electron temperature.

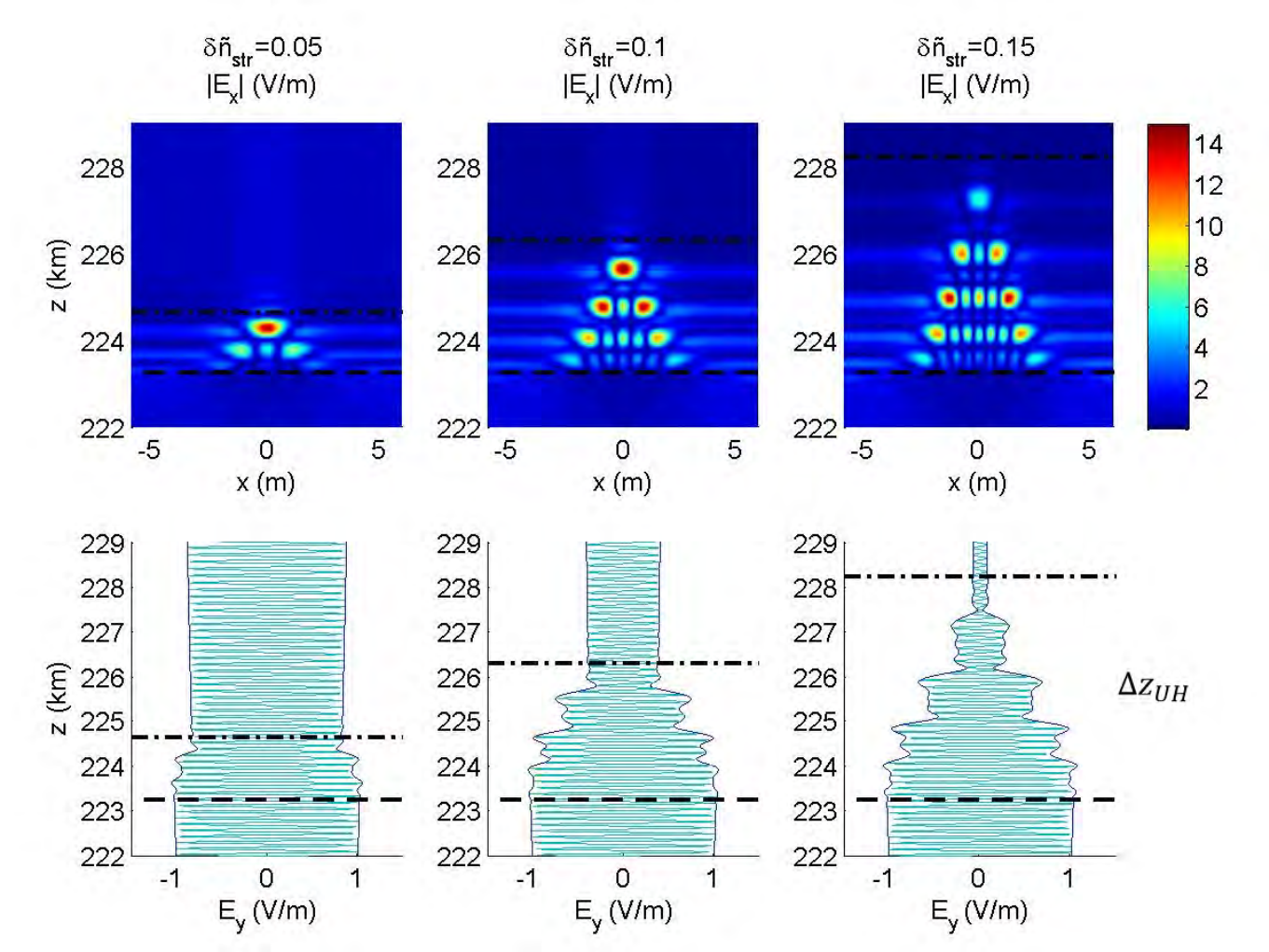

Absorption strongly dependent on striation depth.

Increased absorption with decreasing magnetic field and with increasing plasma length-scale and density of striations.

Expression for transmission coefficient

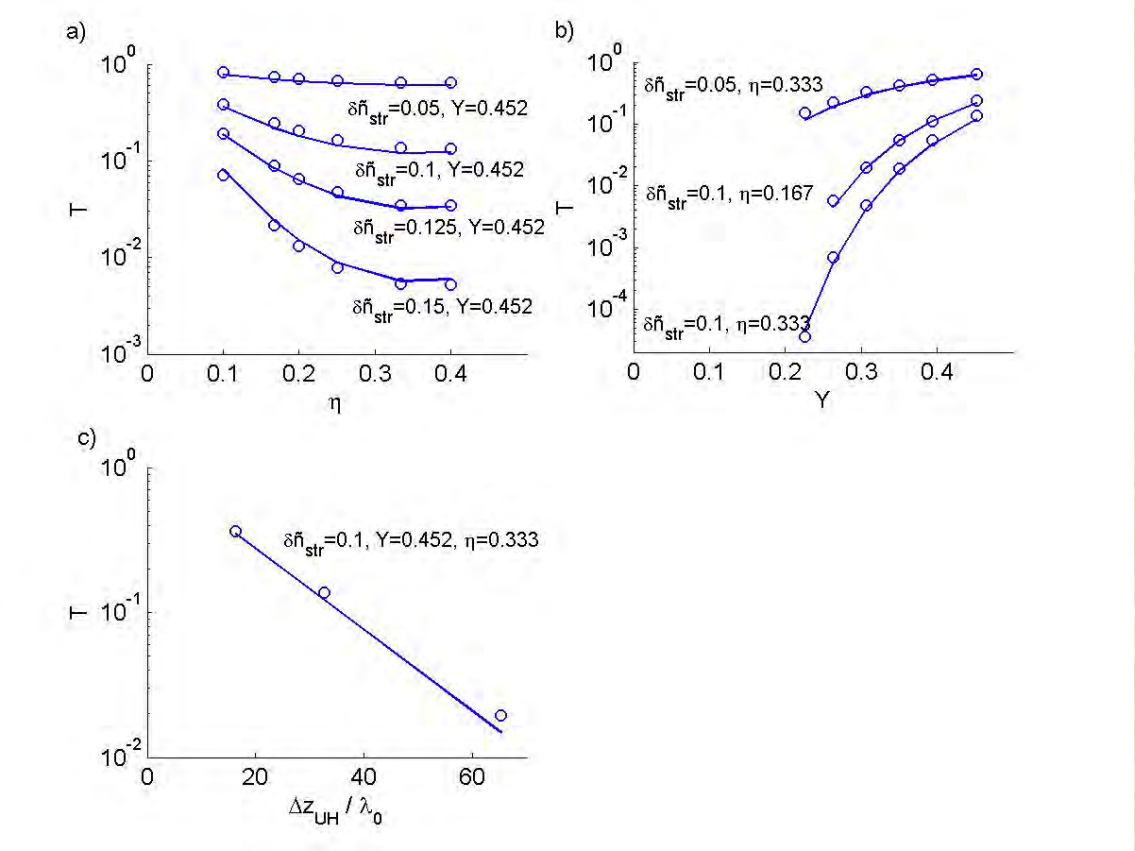

Comparison simulation results (circles) and numerical fit to expression

$$T = \exp\left[-3.24\delta\tilde{n}_{str}\frac{\Delta z_{UH}}{\lambda_0}(\eta - 1.4\eta^2)(\frac{1}{Y} - 1.09)\right], \quad Y = \frac{\omega_{ce}}{\omega_0}$$

Eliasson & Papadopoulos, Geophys. Res. Lett. **42**, 2603 (2015).

Vlasov simulations: Mode conversion to UH waves

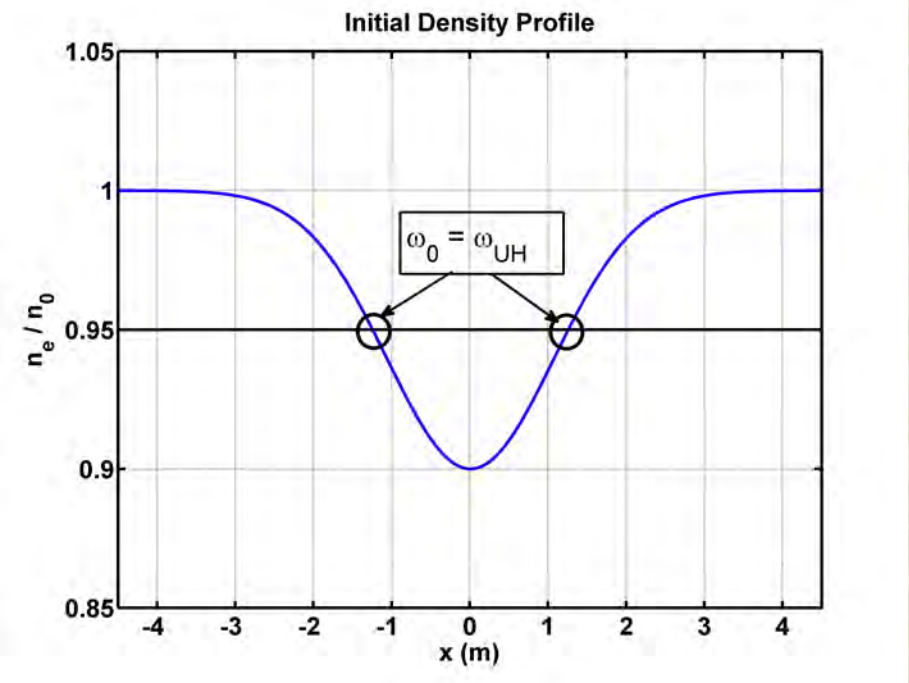

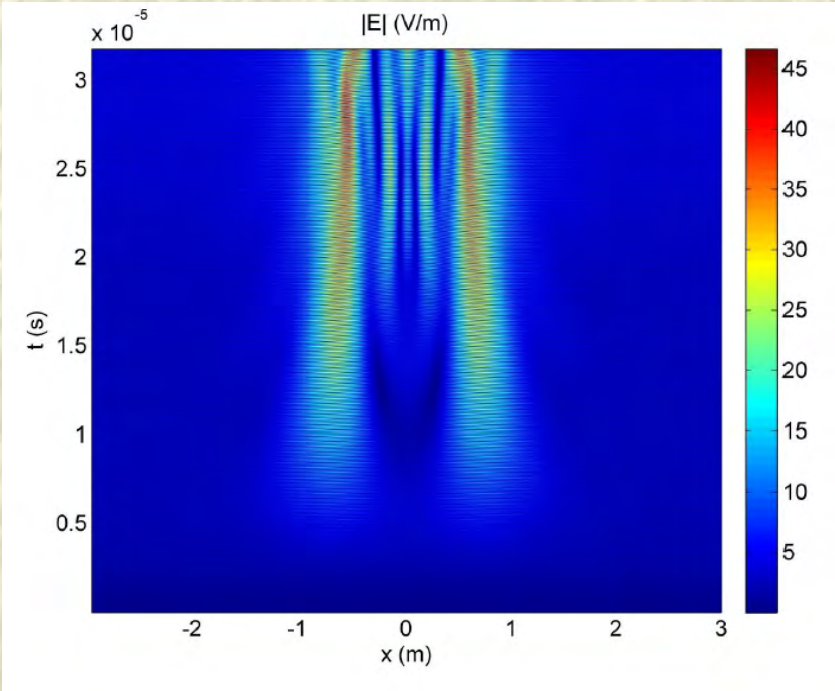

$$\frac{\partial f_\alpha}{\partial t} + v_x \frac{\partial f_\alpha}{\partial x} + \frac{q_\alpha}{m_\alpha}(\widehat{\mathbf{x}}(E + E_{ext}) + \mathbf{v} \times B_0 \widehat{\mathbf{z}}) \cdot \nabla f_\alpha = 0$$

$$\frac{\partial E}{\partial x} = \frac{e}{\epsilon_0} \int (f_i - f_e)\, d^2 v$$

$E_{ext} = E_0 \sin(\omega_0 t)$, Dipole oscillating field representing the O mode.

$E_0 = 2\,\mathrm{V/m}$. Hydrogen ions.

- Mode-converted upper hybrid (UH) waves (~ 50 cm) trapped in striation.

Mode conversion to UH waves, generation of EB waves

$$A = \frac{m_e}{eB_0^2}\frac{\partial E_x}{\partial x}$$ Normalized electric field gradient

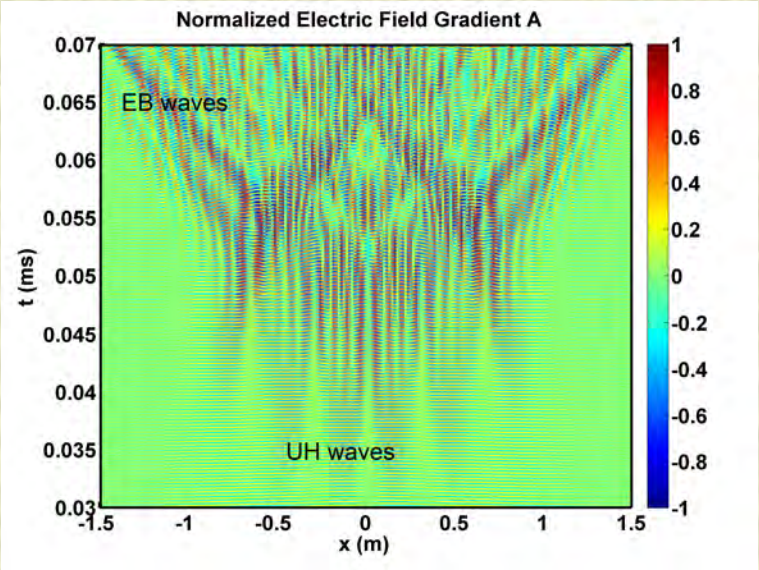

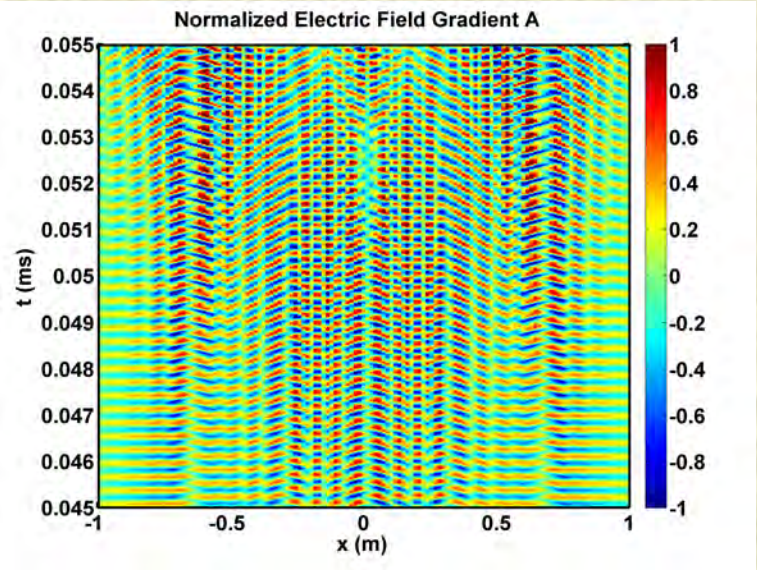

- Short wavelength electron Bernstein (EB) waves (~ 10 cm) excited and leaving the striations.
- Amplitude $|A| > 1$ exceeds threshold for stochastic heating.

A. Najmi, B. Eliasson et al., Radio Science (in press 2016).

Lower hybrid oscillations and electron heating

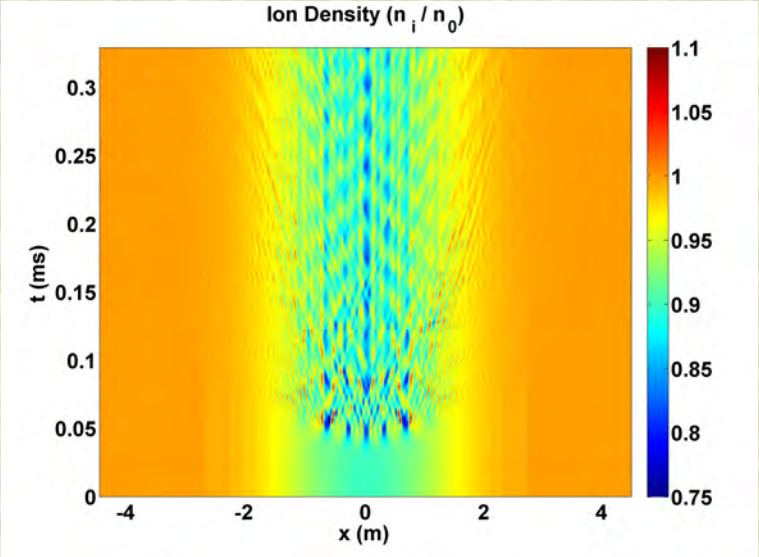

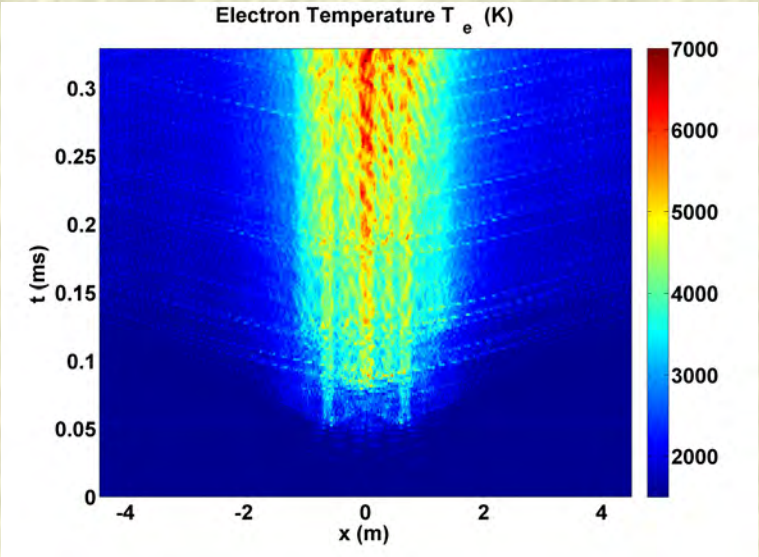

- Lower hybrid (LH) waves form standing wave pattern.
- Electron temperature rises to about 7000 K in the center of the striation.

Electron distribution function at different times

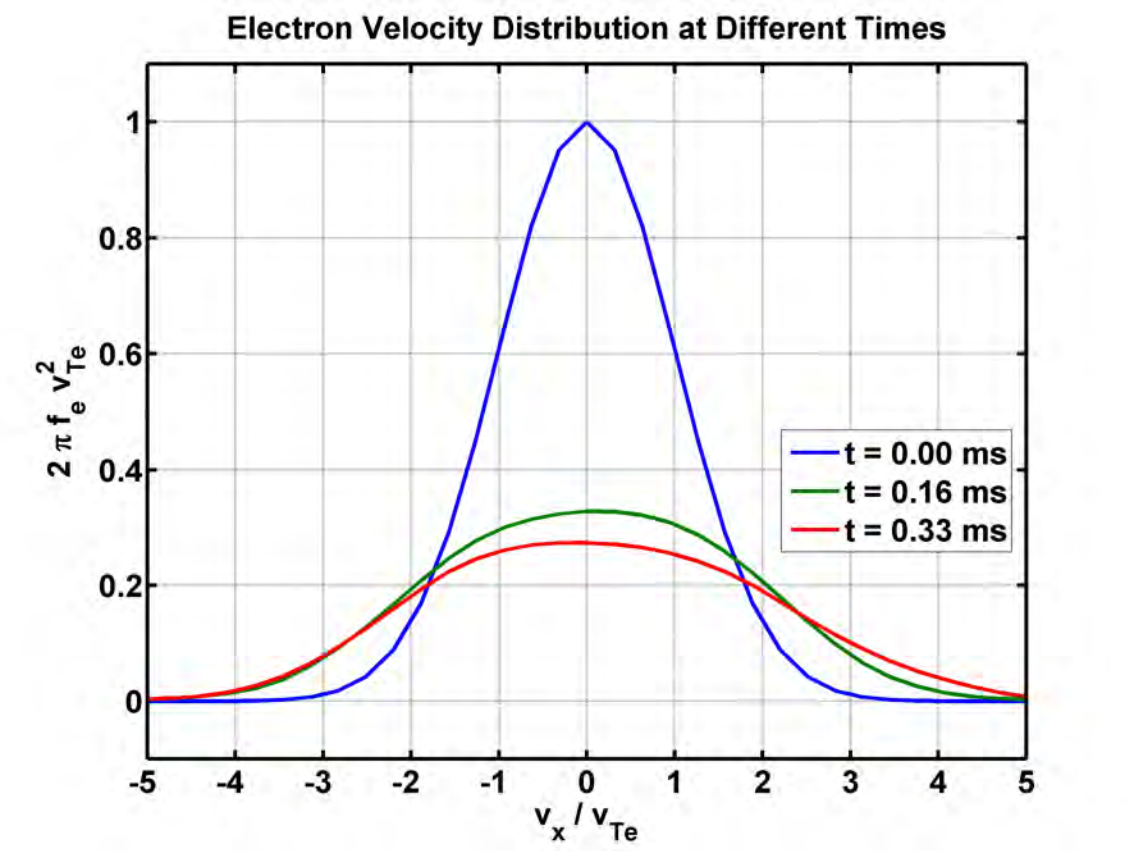

Electron distribution is flattened and widened — bulk heating but no high-energy tails.

Coupling upper hybrid waves to EB and LH waves

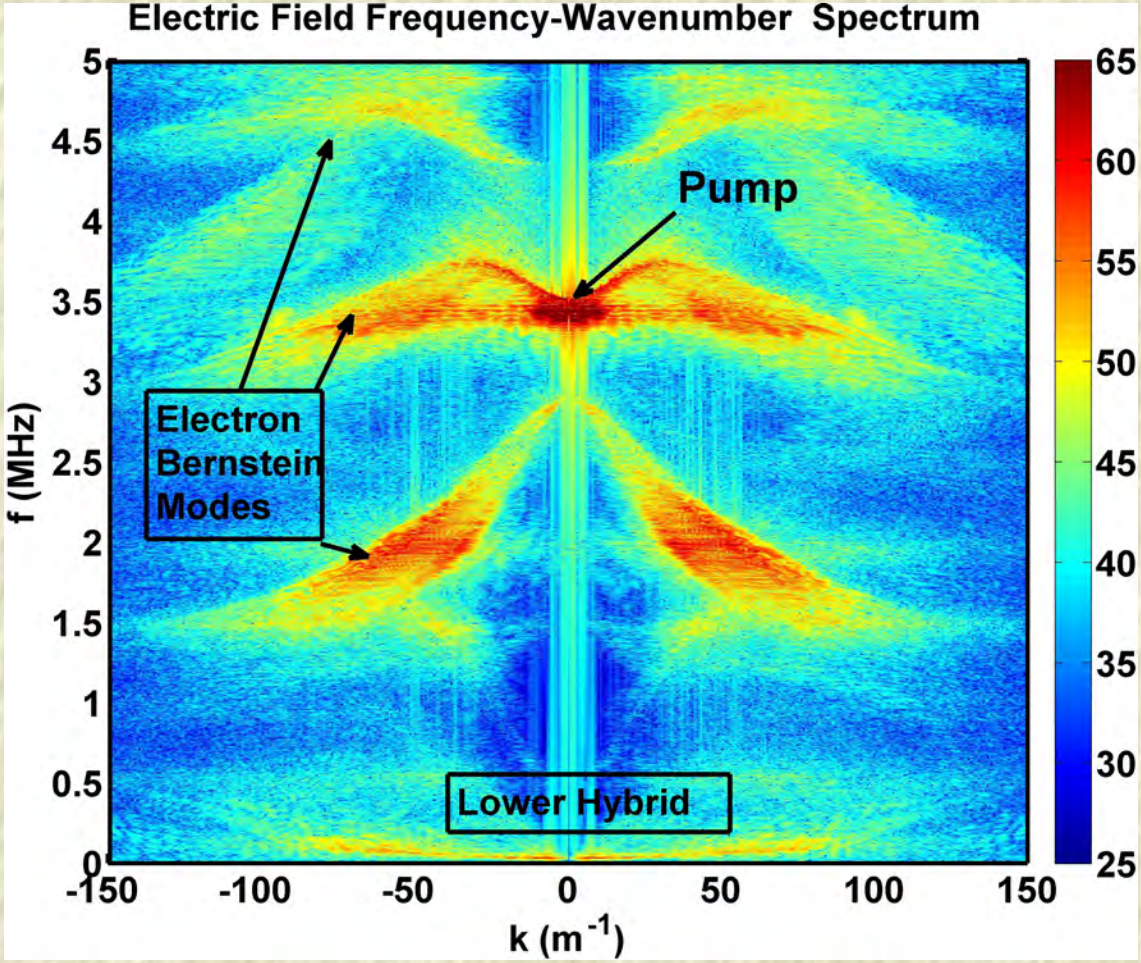

First three electron Bernstein modes and lower hybrid waves are visible.

3-wave decay scenarios

Matching conditions: $\omega_0 = \omega_1 + \omega_2, \quad \mathbf{k}_0 = \mathbf{k}_1 + \mathbf{k}_2$

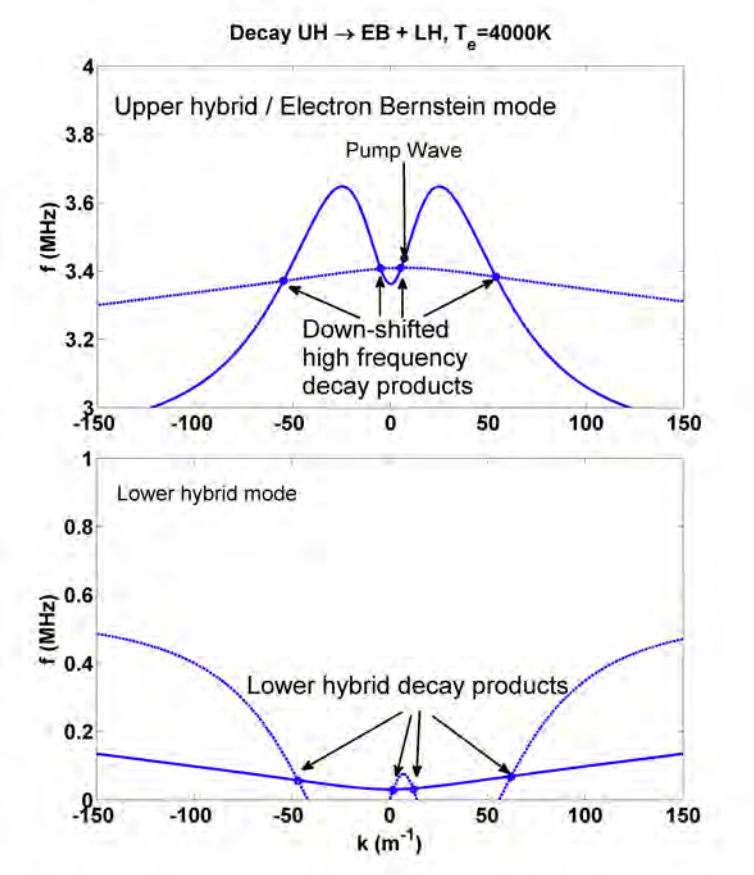

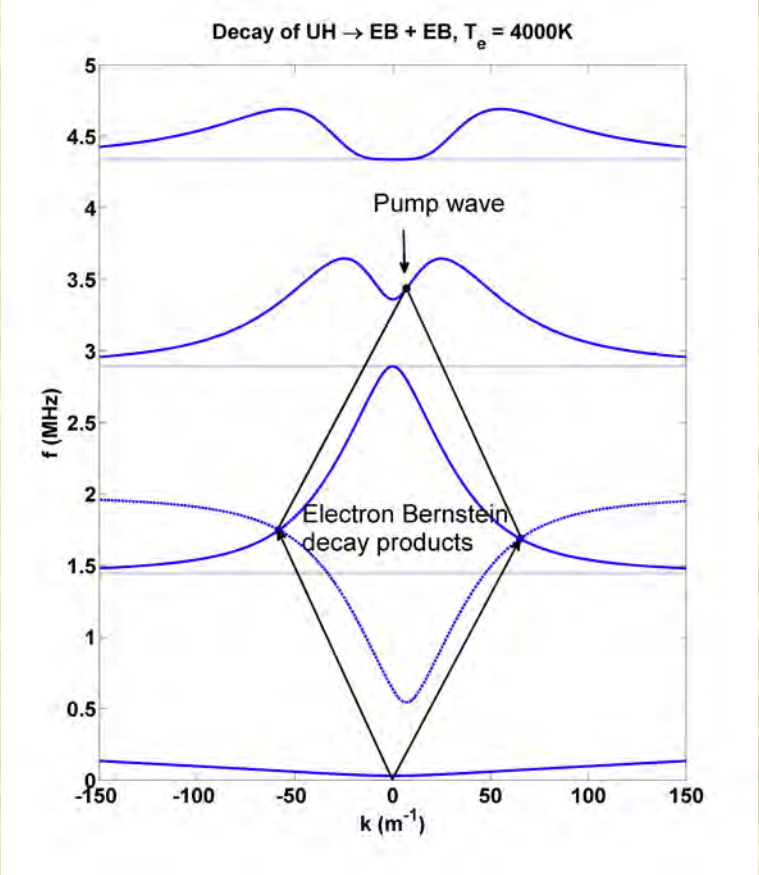

Also potentially 4-wave decay and UH wave collapse taking place.

Preleminary results from 2D Vlasov simulations

Cylindrical striation in 2 dimensions. Run 10 days on 250 processors.

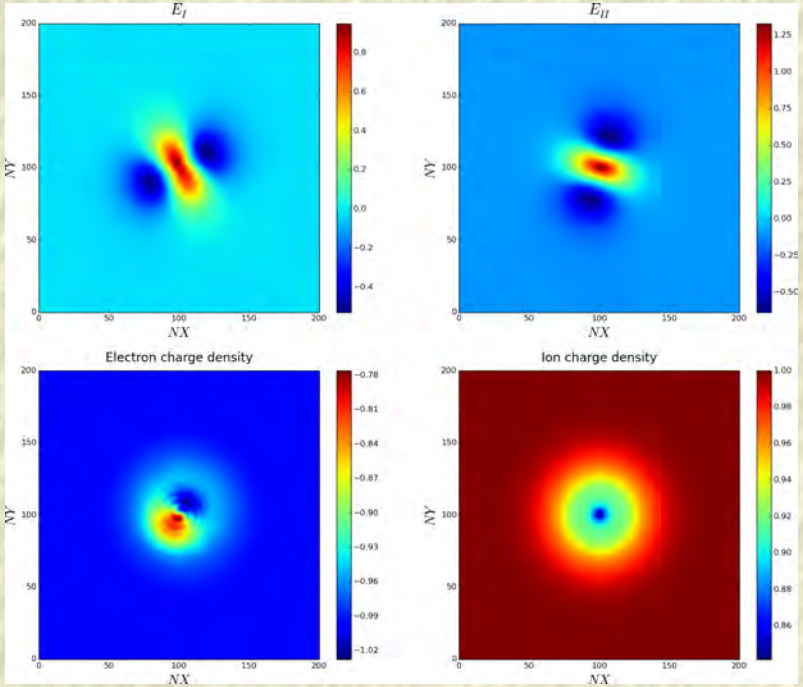

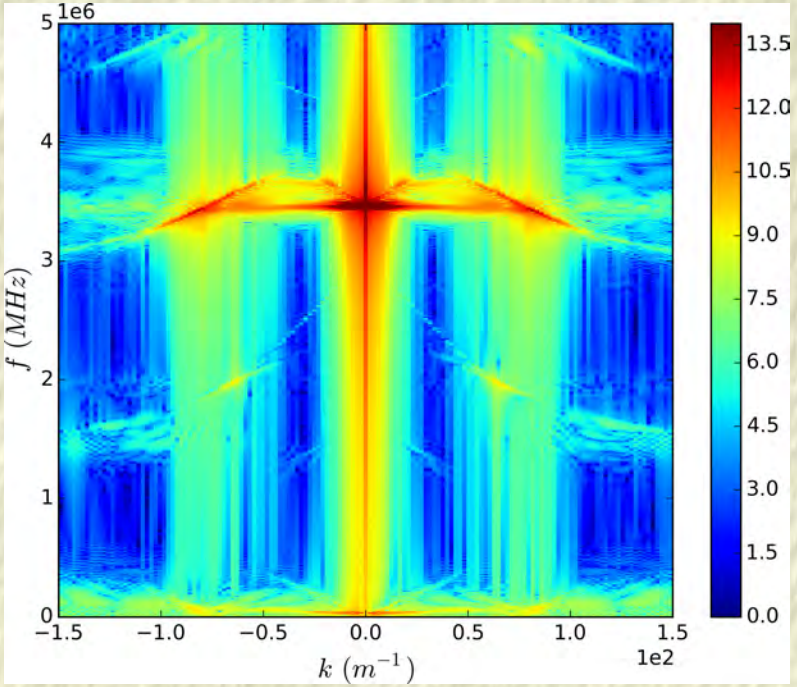

Simulation by David Speirs, U. Strathclyde

Groups of striations may enhance the fields

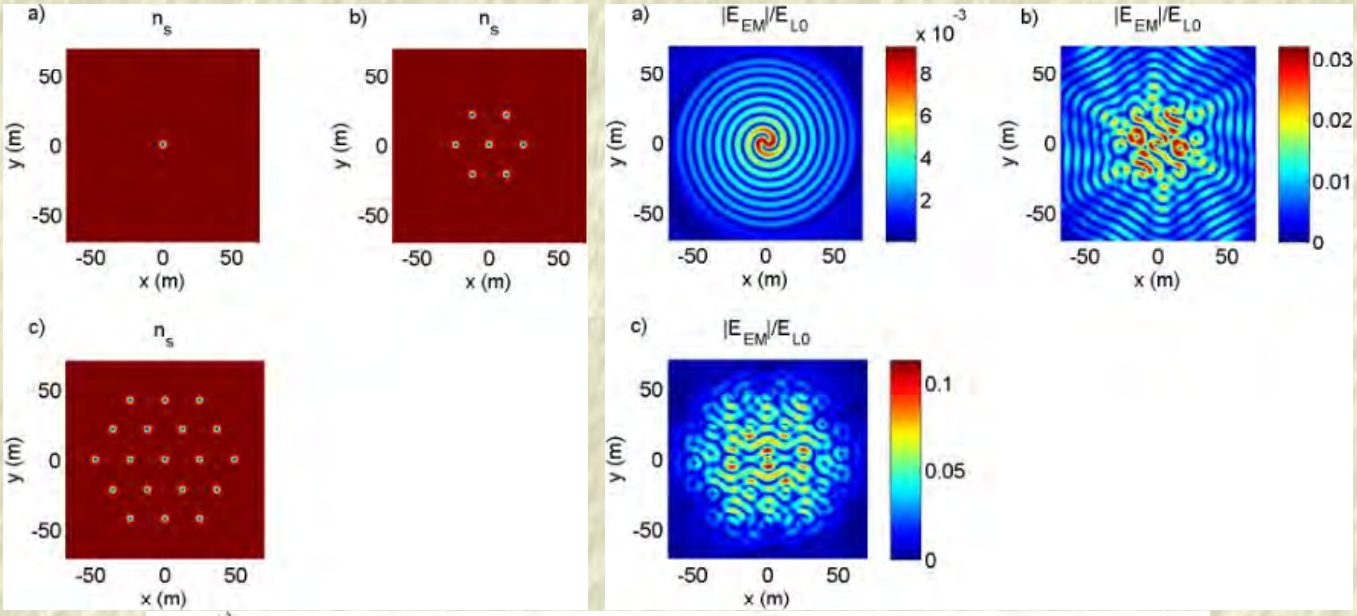

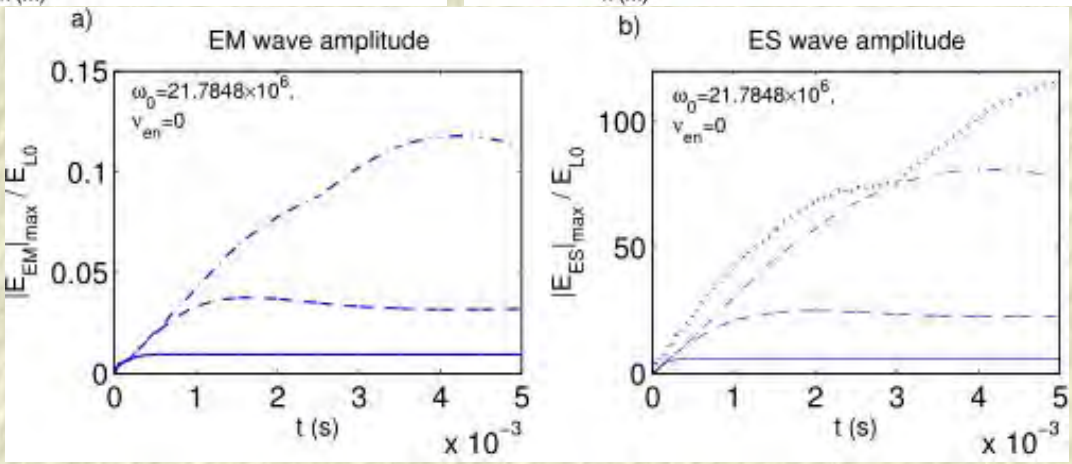

2D fluid simulations: Multiple scatterings of Z mode waves lead to enhanced mode converted UH fields in striations (B. Eliasson & T. B. Leyser, Ann. Geophys. **33**, 1019 (2015))

Comparison: Stochastic heating by an electrostatic wave

Equations of motion for an electron in an electrostatic wave perpendicular to the magnetic field

$$m\frac{d\mathbf{v}^{(j)}}{dt} = -eE_0\sin(kx^{(j)} - \omega t)\widehat{\mathbf{x}} - e\mathbf{v}^{(j)} \times B_0\widehat{\mathbf{z}}, \qquad \frac{dx^{(j)}}{dt} = v_x^{(j)}$$

Normalized model equations

$$\frac{du_x^{(j)}}{dt} = -A\sin(u_y^{(j)} - \Omega t) - u_y^{(j)}, \qquad \frac{du_y^{(j)}}{dt} = u_x^{(j)}$$

where $A = \frac{mkE_0}{eB_0^2}$ and $\Omega = \omega/\omega_{ce}$, $\omega_{ce} = eB_0/m$. Typically $A > 1$ leads to stochastic motion of the particles and to rapid heating of the plasma.

Has been extensively studied in the past:

M. Balikhin et al., Phys. Rev. Lett. **70**, 1259 (1993). $\rightarrow$ Electron heating by shocks
J. McChesney et al., Phys. Rev. Lett., **59**, 1436 (1987). $\rightarrow$ Ion heating by drift waves
C. F. F. Karney, Phys. Fluids **21**, 1584 (1978). $\rightarrow$ Ion heating by lower hybrid waves

A. Fukuyama et al., Phys. Rev. Lett. **38**, 701 (1977) $\rightarrow$ Ion heating near gyroharmonics.

Electron distribution function

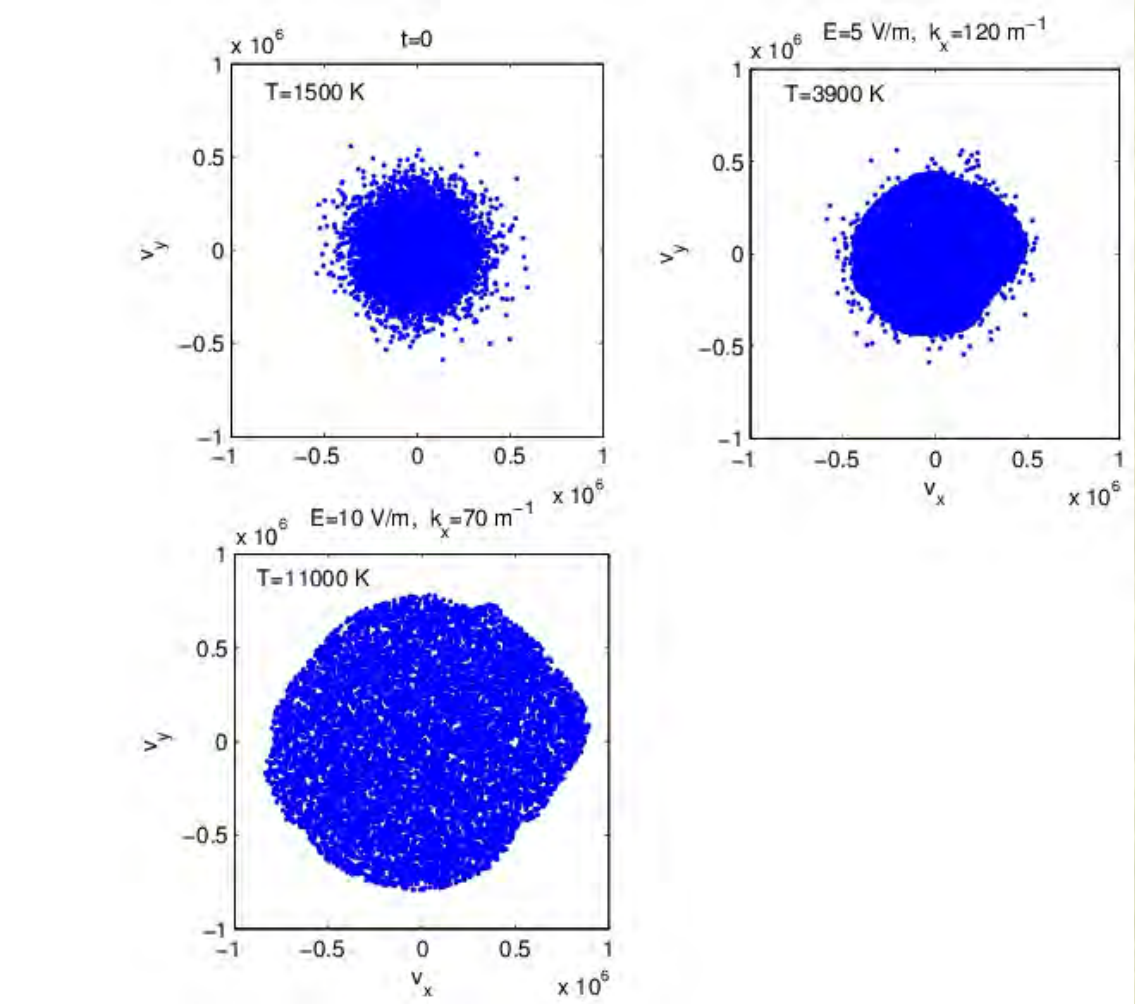

Test particle simulations 10^4 particles, simulation times a few hundred gyroperiods. Flat-topped electron distributions are developed. No suprathermal tails.

Temperature dependence on amplitude

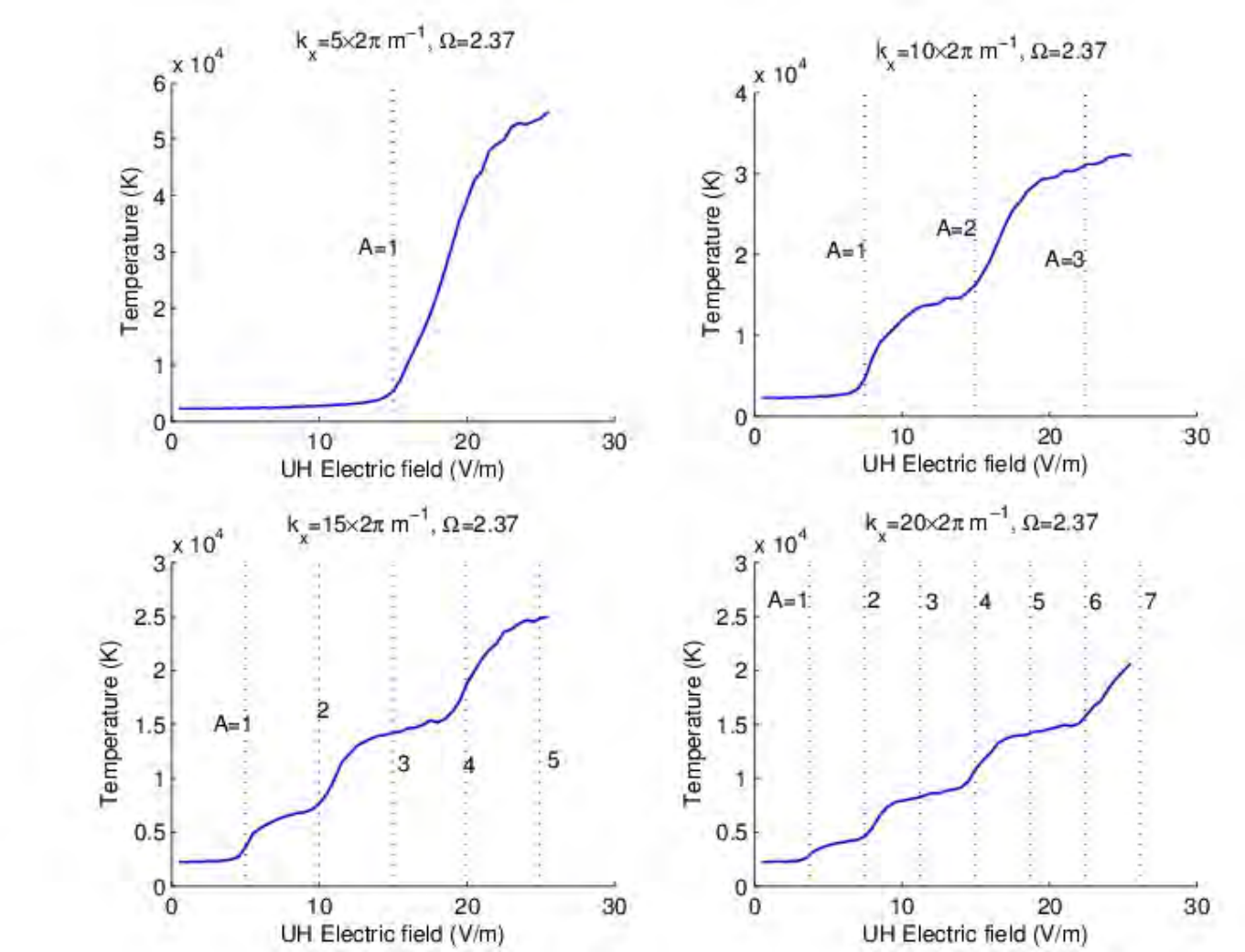

Each point on the curve represents one test particle simulation.

Temperature dependence on frequency

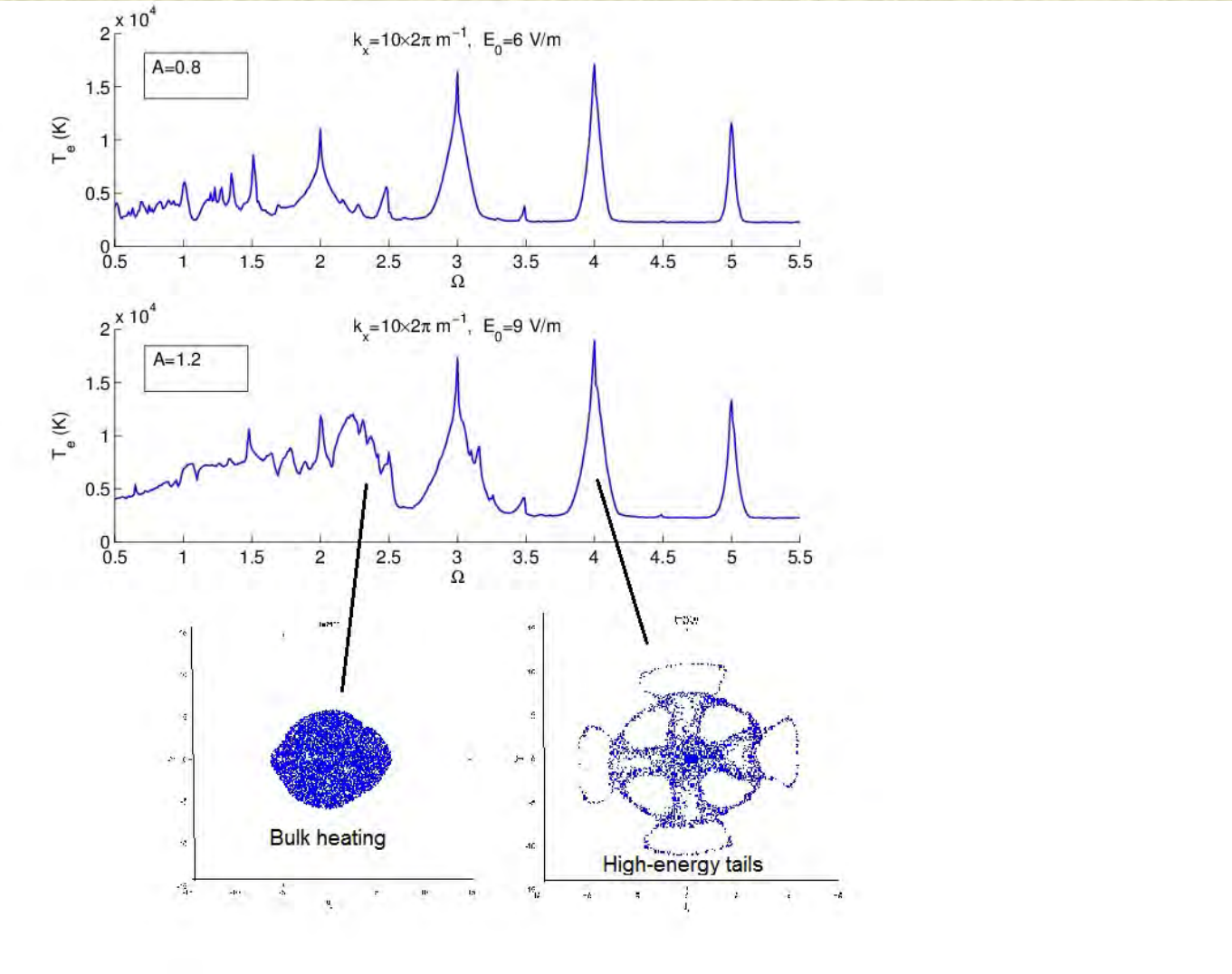

Temperature peaks near cyclotron harmonics. Rises between cyclotron harmonics for $A > 1$.

Electron acceleration by strong Langmuir turbulence

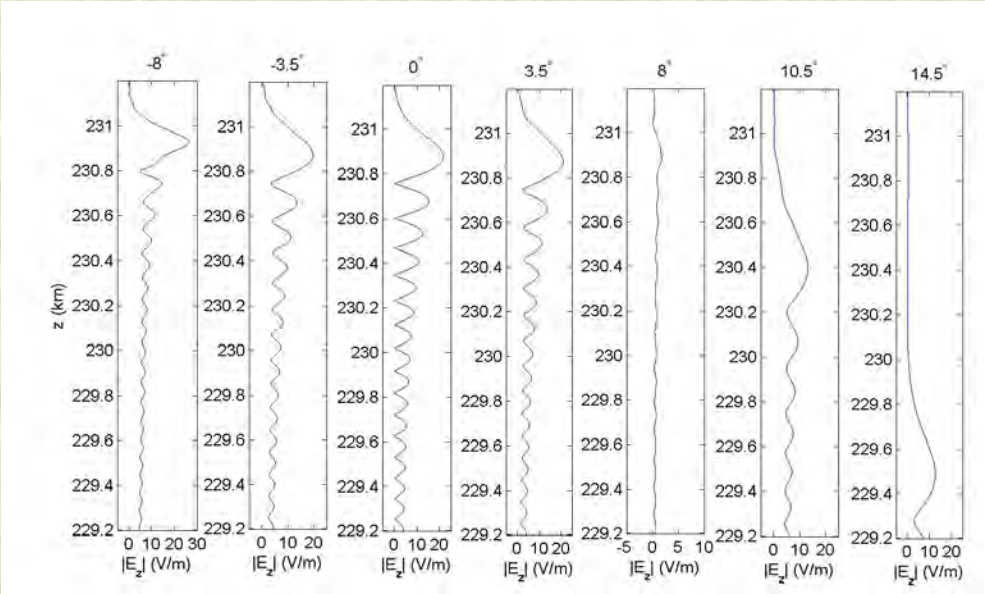

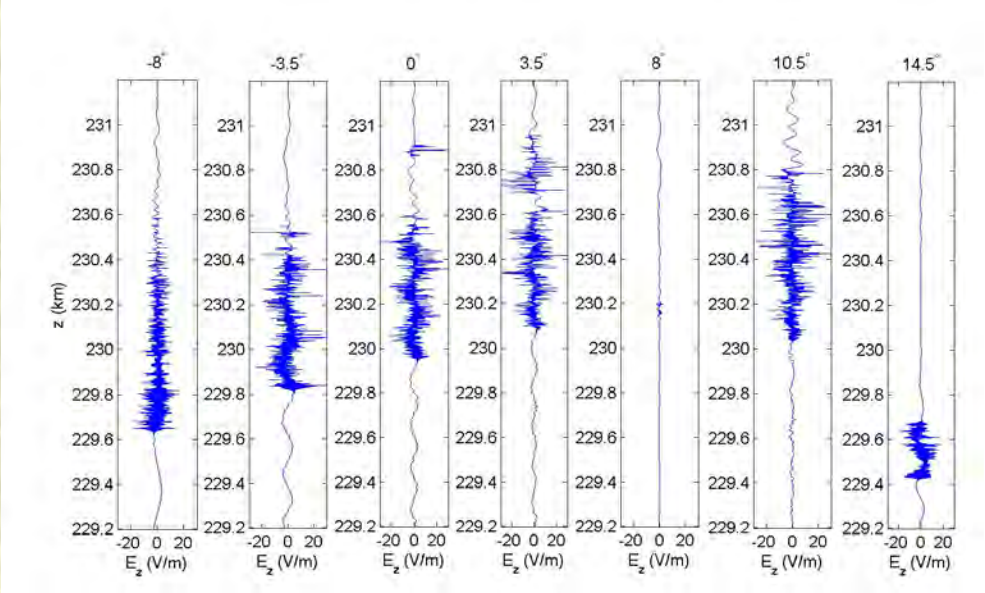

Electromagnetic wave breaks up into small-scale electromagnetic turbulence via parametric instabilities creating strong Langmuir turbulence

Most important:
4-wave oscillating two-stream instability creating localized wave envelopes accelerating electrons

OTSI and PDI

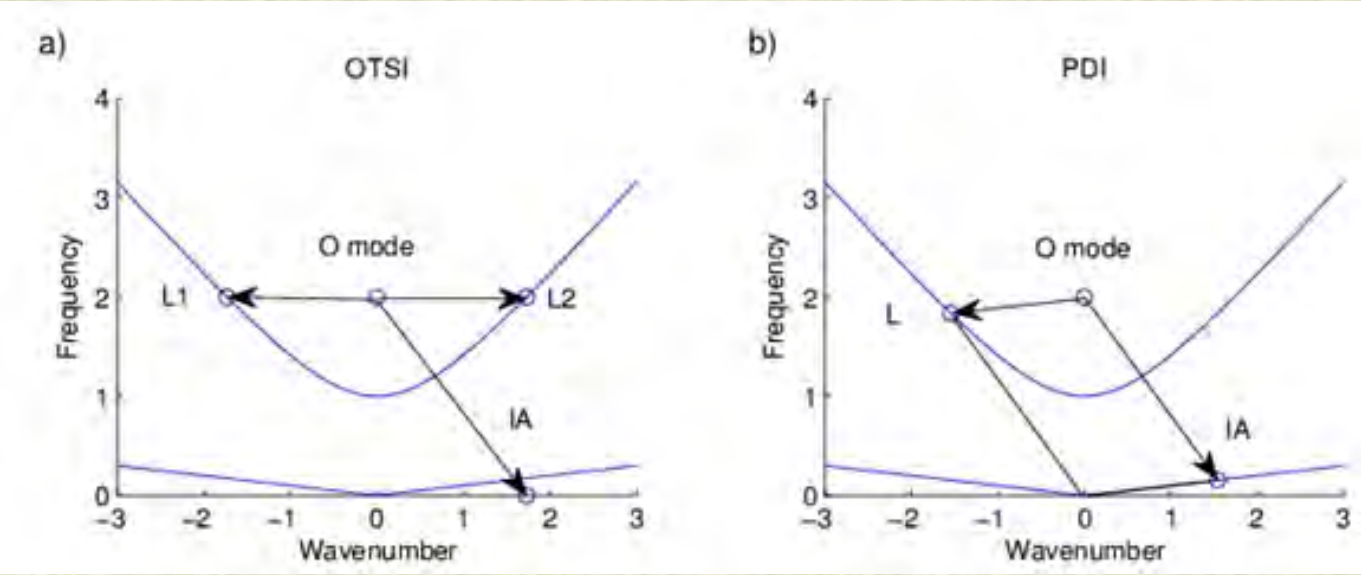

Sketch of the 4-wave oscillating two-stream instability (OTSI) and 3-wave parametric decay instability (PDI) coupling HF Langmuir (L) waves and low-frequency ion-acoustic (IA) waves. Combination of instability and mode conversion EM to ES waves!

Growth-rate ($\omega_1 = \omega_R + i\gamma$) dispersion relation:

$$-\omega_1^2 - 2i\gamma_i\omega_1 + C_s^2 k_1^2 = \frac{\epsilon_0 E_0^2 \omega_p e^2 k_1^2}{4 m_i n_0}\left(\frac{1}{D_+} + \frac{1}{D_-}\right)$$

where $D_\pm = -(\pm\omega_0 + \omega_1)^2 - i\nu_e(\pm\omega_0 + \omega_1) + 3v_{Te}^2 k_1^2 + \omega_{pe}^2$, and ν_i and ν_e are ion and electron damping rates due to collisions and Landau damping.

Eliasson & Papadopoulos, J. Geophys. Res. 121, 2727 (2016).

Growth-rates and real frequencies of the OTSI and PDI

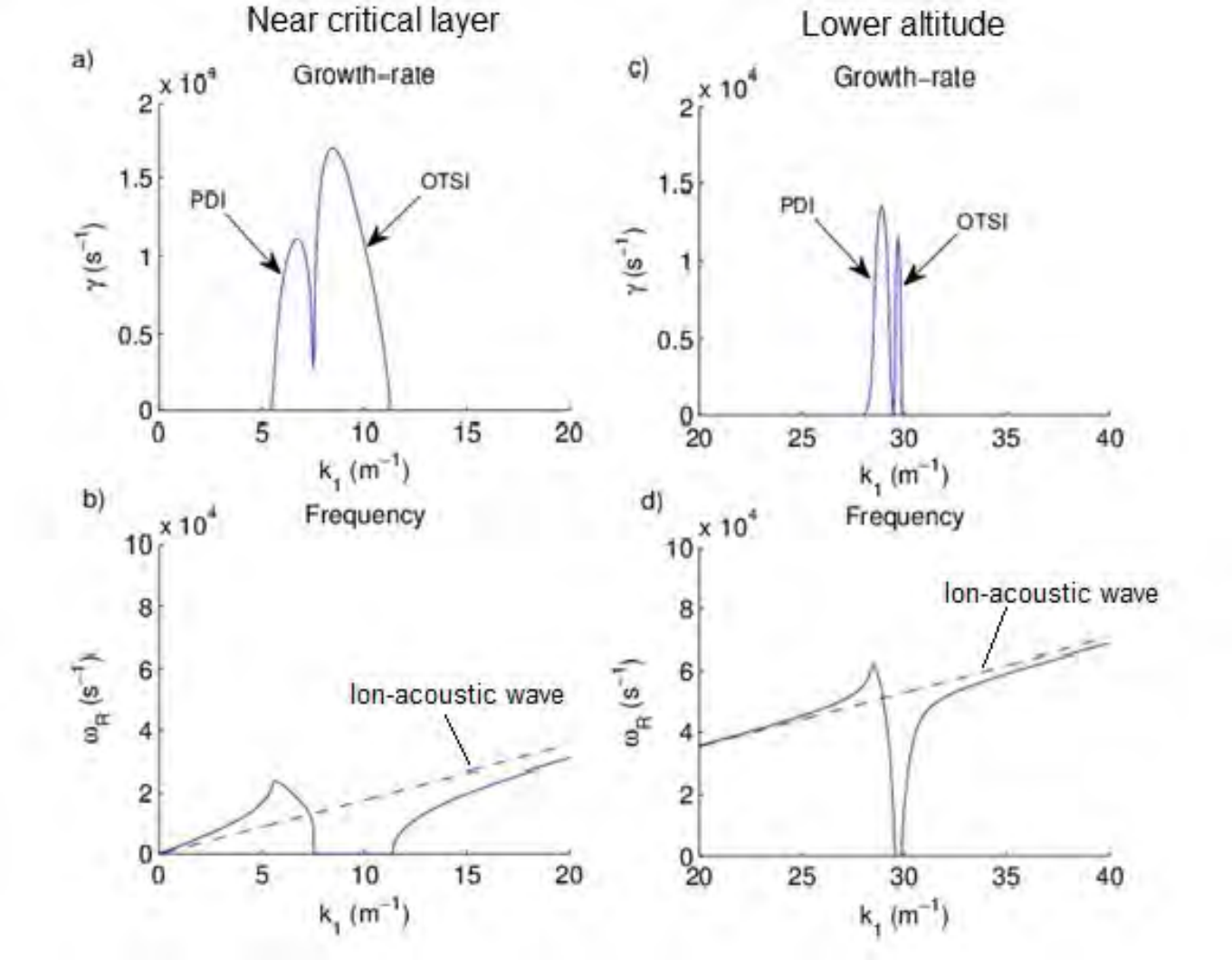

OTSI purely growing; PDI creates propagating ion acoustic waves. Larger frequency mismatch $\omega_0 - \omega_{pe}$ at lower altitudes, eventually quenching due to Landau damping.

Electron acceleration by plasma waves

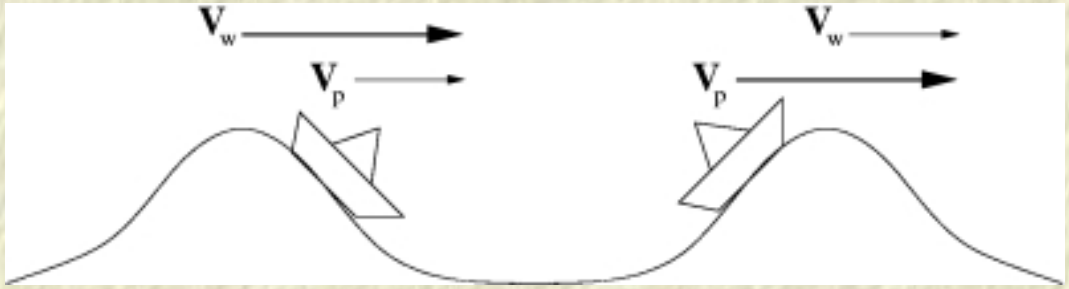

Fast electrons passing over a solitary structure feels a DC electric field. Many passages give random walk and diffusion of electron velocity.

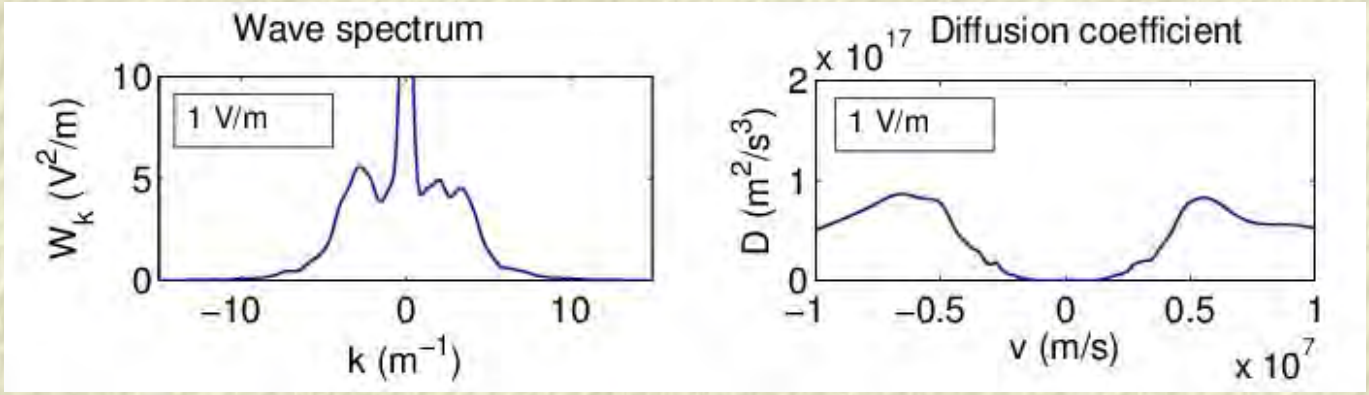

Fokker-Planck equation and diffusion coefficient.

$$\frac{\partial f}{\partial t} + v\frac{\partial f}{\partial z} = \frac{\partial}{\partial v} D(v) \frac{\partial f}{\partial v}, \qquad D(v) = \frac{\pi e^2}{m_e^2} \frac{W_k(\omega, k)}{|v|}, \quad k = \frac{\omega}{v}.$$

Sagdeev & Galeev (1969); Stix, *Waves in Plasmas* (1992).

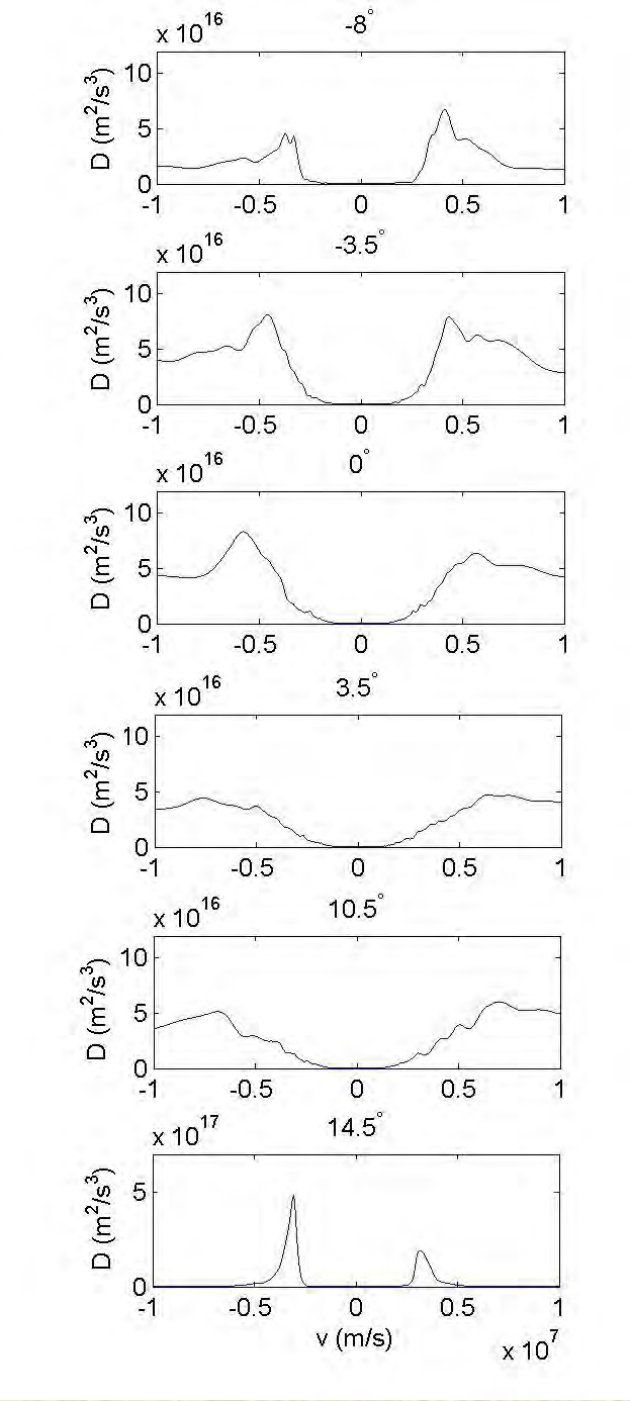

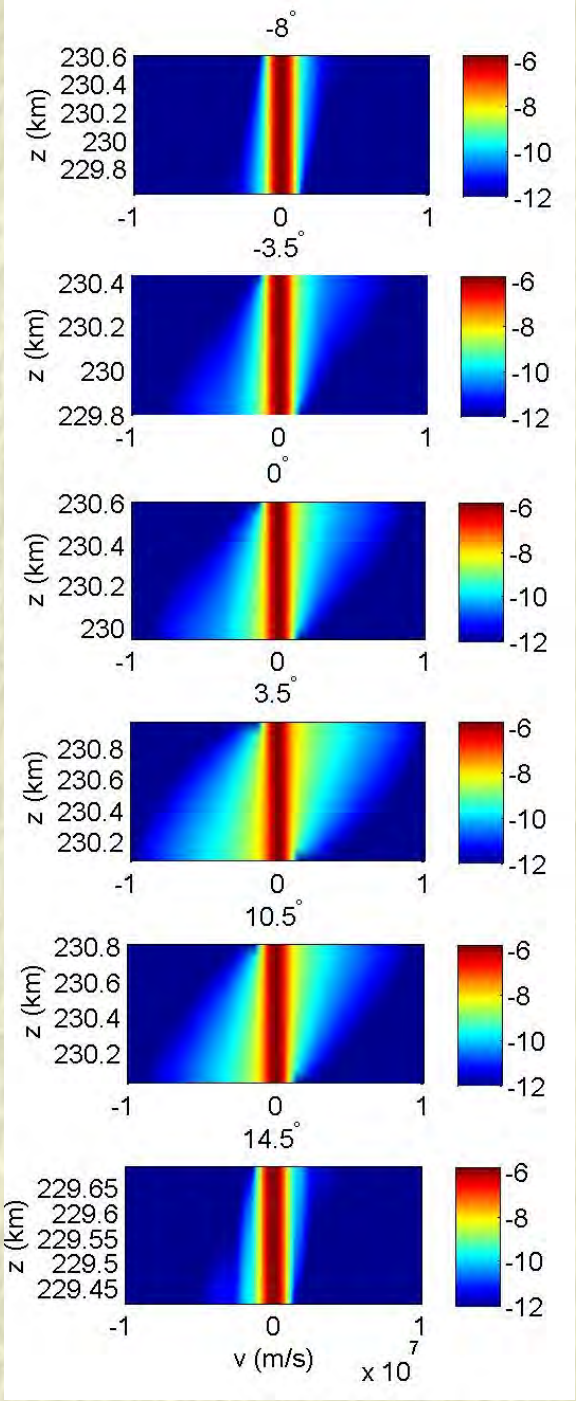

Diffusion coefficients and Fokker-Planck solutions (velocity distribution) for different angles of incidence

Most significant acceleration at $3.5°$ **and** $10.5°$

Physics at different length-scales

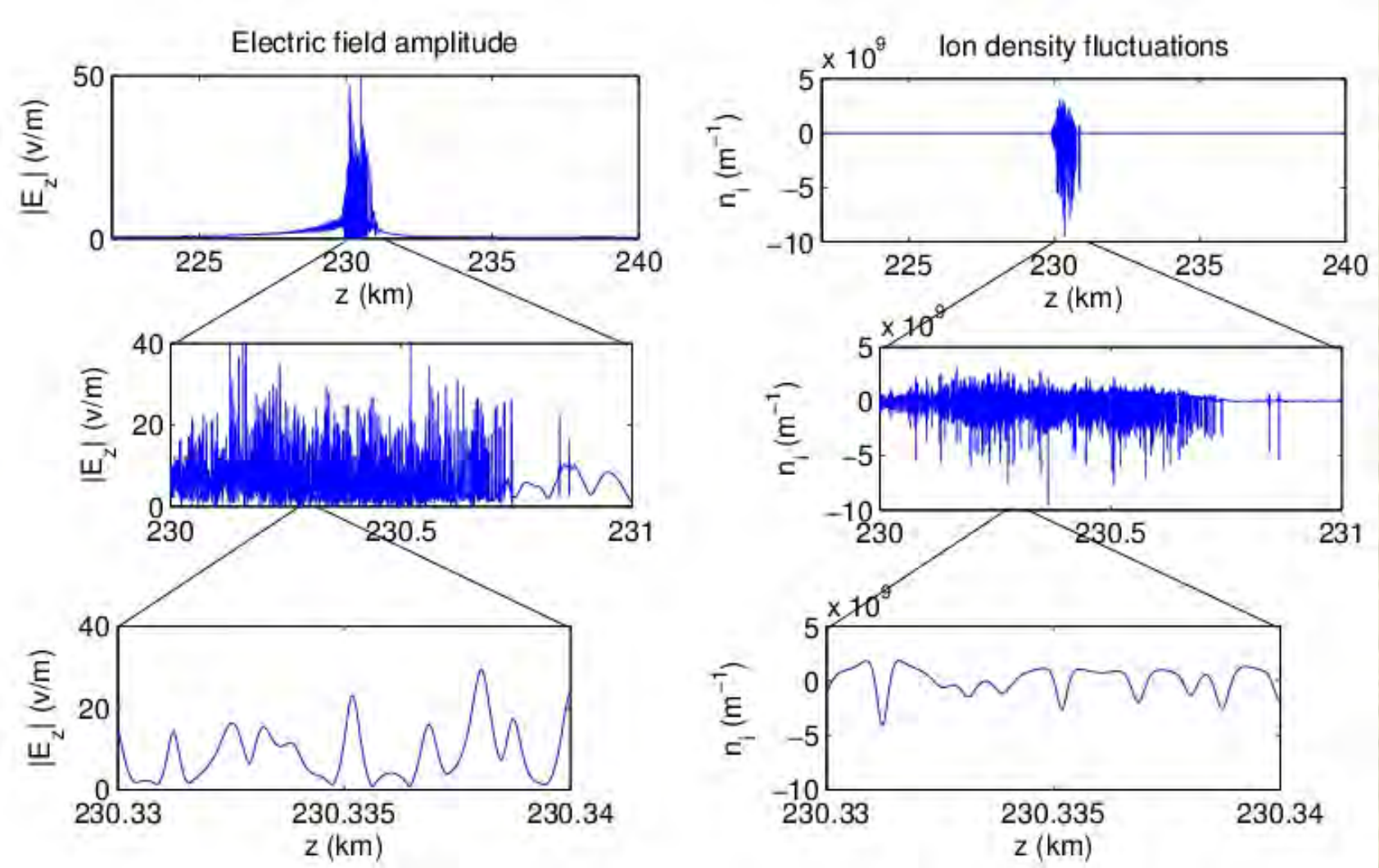

Small-scale strong Langmuir turbulence: few tens of centimetre structures.

Large amplitude electric field envelopes trapped in density cavities.

Dynamical model for ionization and recombination

- Transport model for energetic electrons through the ionosphere.
- Ionization due to collisions between high energy electrons and neutral atoms.
  - Ionization of atomic and molecular oxygen and nitrogen by high-energy electrons
    ($O + e^- \rightarrow O^+ + 2e^-$ and $O_2 + e^- \rightarrow O_2^+ + 2e^-$, etc.)
  - Production of molecular oxygen ions and nitrogen monoxide ions via charge exchange collisions
    ($O^+ + O_2 \rightarrow O_2^+ + O$ and $O^+ + N_2 \rightarrow NO^+ + N$)
  - Dissociative recombination between electrons and molecular ions
    $O_2^+ + e^- \rightarrow 2O$ and $NO^+ + e^- \rightarrow N + O$).

Simulated descending artificial ionospheric layer

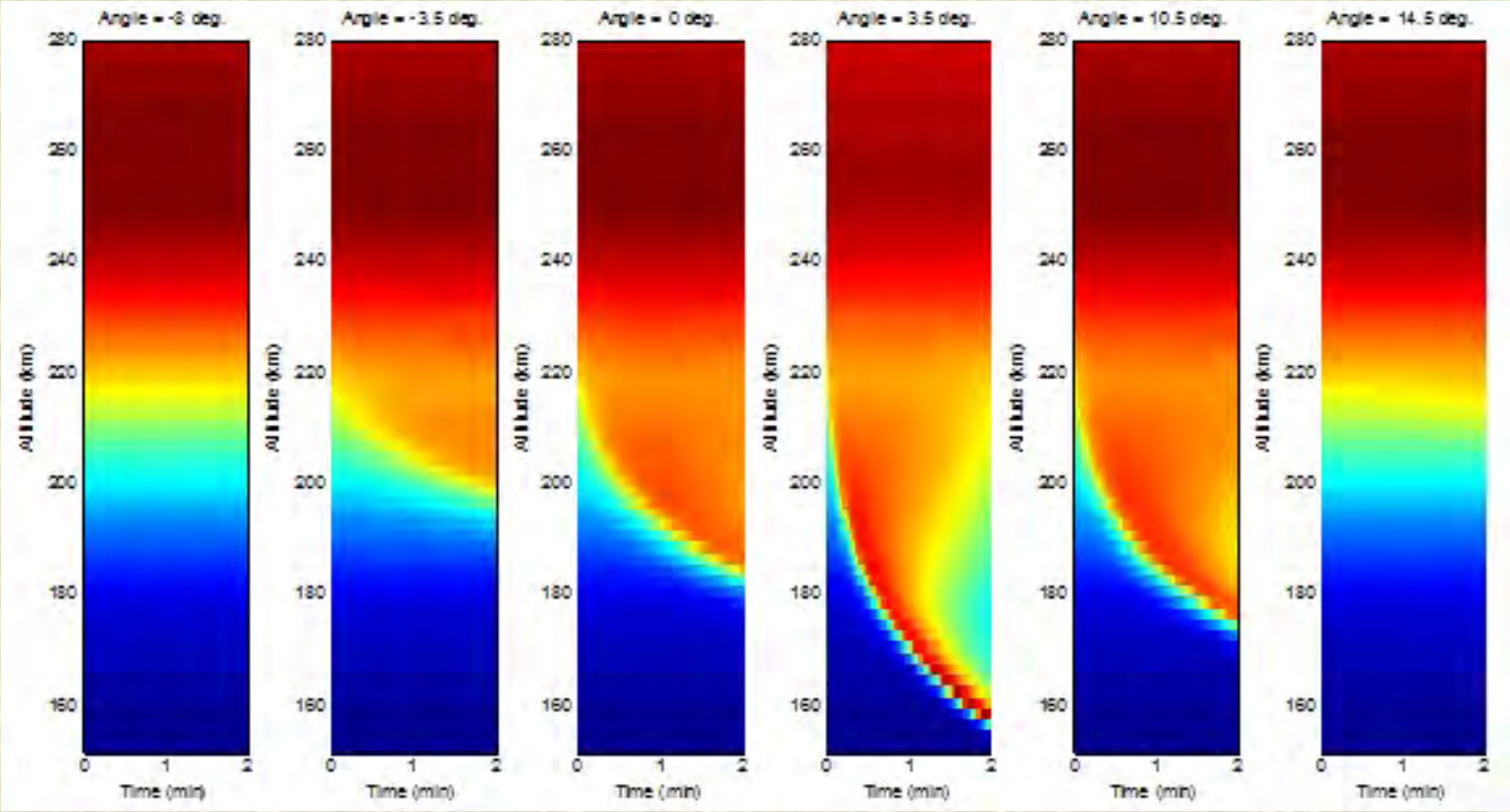

Simulations by Xi Shao, U. Maryland

- Ionization fronts descending from about 200 km to 150 km in a few minutes, consistent with the experiments.
- Physics on microsecond $\rightarrow$ millisecond $\rightarrow$ several minutes timescales!

Electromagnetic cyclotron (whistler) instability

EMEC/Whistler instability, bi-Kappa distribution function

$$f(v_\parallel, v_\perp) = \frac{1}{\pi^{3/2}\theta_\perp^2\theta_\parallel}\frac{\Gamma(\kappa+1)}{\kappa^{3/2}\Gamma(\kappa-1/2)}\left(1+\frac{v_\parallel^2}{\kappa\theta_\parallel^2}+\frac{v_\perp^2}{\kappa\theta_\perp^2}\right)^{-\kappa-1},$$

where κ is the power index, and the parallel and perpendicular thermal speeds $\theta_\parallel$ and $\theta_\perp$ are defined in terms of the respective kinetic temperatures $T_\parallel$ and $T_\perp$ via

$$T_\parallel = \frac{m_e\theta_\parallel^2}{2k_B}\frac{\kappa}{\kappa-3/2}, \qquad T_\perp = \frac{m_e\theta_\perp^2}{2k_B}\frac{\kappa}{\kappa-3/2}.$$

The linear dispersion relation EMEC-whistler instability parallel propagation along the background magnetic field

$$\frac{k^2c^2}{\omega_p^2} = \frac{T_\perp}{T_\parallel} - 1 + \frac{(\omega-\omega_{ce})T_\perp/T_\parallel + \omega_{ce}}{k\sqrt{2k_BT_\parallel/m_e}\sqrt{1-3/(2\kappa)}}\,Z_\kappa\left(\frac{\omega-\omega_{ce}}{k\sqrt{2k_BT_\parallel/m_e}\sqrt{1-3/(2\kappa)}}\right)$$

in terms of the bi-Kappa dispersion function

$$Z_\kappa(\xi) = \frac{1}{\pi^{1/2}\kappa^{1/2}}\frac{\Gamma(\kappa)}{\Gamma(\kappa-1/2)}\int_{-\infty}^{\infty}dx\,\frac{(1+x^2/\kappa)^{-\kappa}}{x-\xi}, \quad \Im(\xi)>0.$$

Electromagnetic cyclotron (whistler) instability

Comparison theory and Vlasov simulations (1 spatial + 3 velocity dimensions)

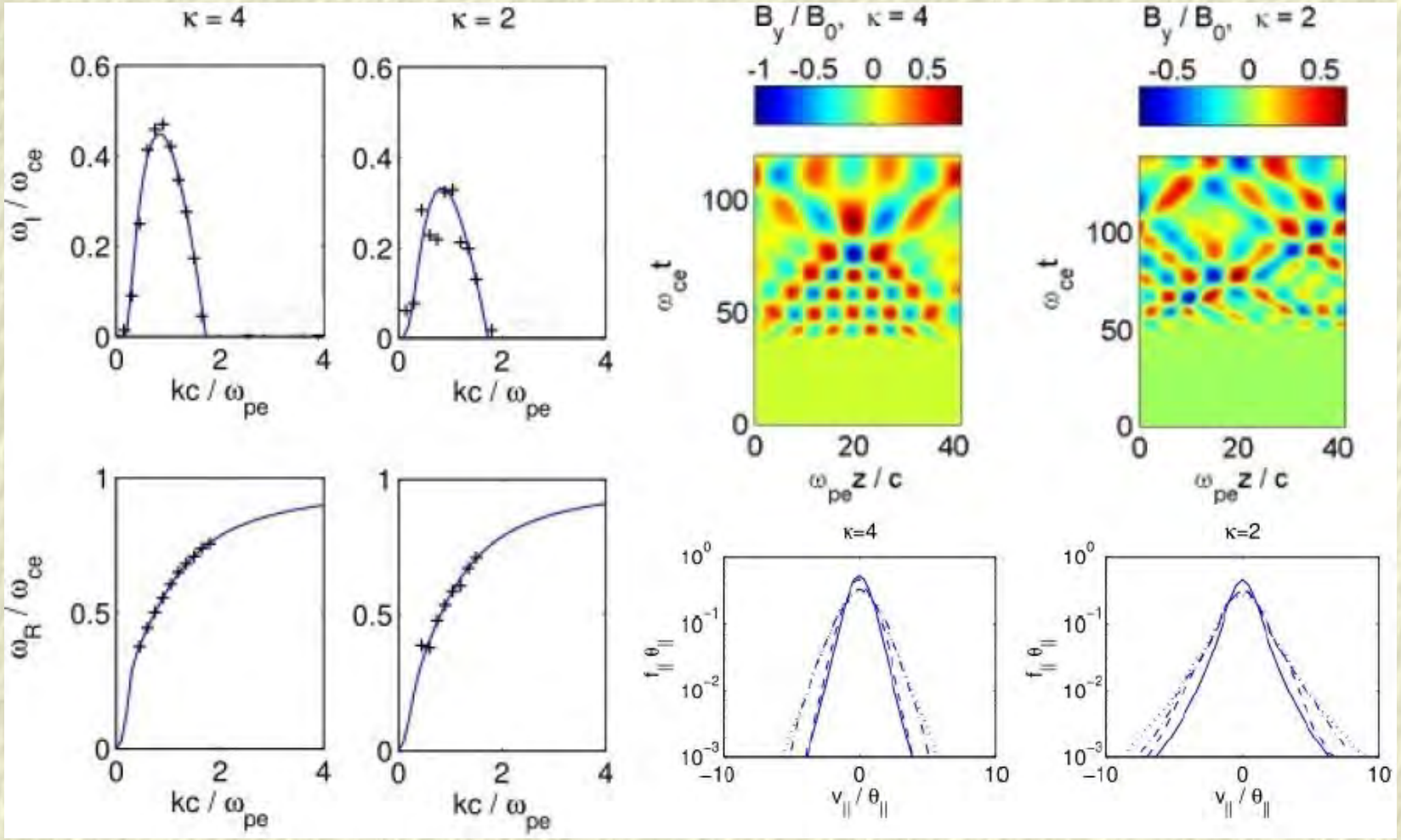

Eliasson & Lazar, Phys. Plasmas **22**, 062109 (2015)

Development of Vlasov codes

- The Fourier method has been developed in $1+1$, $2+2$ and $3+3$ dimensions.
  - Electromagnetic and electrostatic options
  - B. Eliasson, Transport Theory and Statistical Physics **39**, 387 (2011) [Proceedings of Vlasovia 2009]

- Fully parallelized in $1+1$ and $2+2$ dimensions (using MPI), planned parallelization in $3+3$ dimensions.
  - B. Eliasson, Comput. Phys. Commun. **170**, 205 (2005).
  - L. K. S. Daldorff & B. Eliasson, Parallel Comput. **35**, 109 (2009).

- Various versions, including $1+1$ and $3+3$ hybrid-Vlasov, $2+2$ Darwin, $2+2$ Wigner solvers.

Summary

- Formation of descending aurora/ionization fronts in experiments. Ionosphere used as a plasma laboratory!
- Wave-wave interactions: Mode conversion and parametric instabilities creating short wavelength electrostatic waves
- Wave-particle interactions leading to acceleration of electrons
  - Stochastic heating. Large amplitude electron Bernstein waves perpendicular to the magnetic field makes the particle orbits unstable, leading to bulk heating of electrons
  - ”Quasilinear” acceleration: Diffusion in velocity space by strong Langmuir turbulence along magnetic field leading to the formation of high-energy tails.
- Vlasov simulations used to electron heating by Bernstein waves
- Physics on different length-scales tens of km to 0.1 m, and time-scales microseconds to minutes.